

Encapsulation of Hydrophobic Drugs in a Copolymer: Glass Transition Behavior and Miscibility Evaluation

R. Jayachandra Babu,¹ Witold Brostow,^{2,3} Oladiran Fasina,⁴ Ioannis M. Kalogeras,⁵
Sateeshkumar Sathigari,¹ Aglaia Vassilikou-Dova⁵

¹ Department of Pharmacal Sciences, Harrison School of Pharmacy, Auburn University, Auburn, Alabama 36849

² Laboratory of Advanced Polymers and Optimized Materials (LAPOM), Department of Materials Science and Engineering, and Center for Advanced Research and Technology (CART), University of North Texas, Denton, Texas 76203-5017

³ Department of Physics, University of North Texas, Denton, Texas 76203-5017

⁴ Department of Biosystems Engineering, Auburn University, Alabama 36849

⁵ Solid State Physics Section, Department of Physics, University of Athens, Panepistimiopolis, Zografos 157 84, Greece

The knowledge of glass transition temperatures T_g in drug + polymer systems is indispensable for drug encapsulation. T_g values as a function of composition make possible the determination whether a given polymer is miscible or compatible with the drug and whether the polymer will provide release of the drug into organism within an acceptable rate range. We have used differential scanning calorimetry and Fourier-transform infrared spectroscopy to evaluate miscibility in solid dispersions of the drugs carvedilol, itraconazole, nevirapine, and nimodipine in the pharmaceutical grade copolymer poly(vinyl pyrrolidone-co-vinyl acetate) (PLS-630 Copovidone). Successful drug encapsulation is discussed in terms of thermophysical behavior (suppression of crystallization, negative excess volumes of mixing) and intermolecular interactions (concentrations of proton donating/accepting groups) in drug + polymer systems. Several equations were applied to the complex s-shaped $T_g(\phi)$ patterns obtained (ϕ being the mass fraction of the drug). The best agreement of calculations with experiment is achieved using a recently proposed three-parameter equation, symmetric with respect to the equal concentration of both components. POLYM. ENG. SCI., 51:1456-1465, 2011. © 2011 Society of Plastics Engineers

INTRODUCTION

Currently, a major research focus of pharmaceutical industry consists in improved ways of dealing with the existing drug molecules—rather than in costly search for new chemical entities. It has been clearly established that absorption of a drug by a human organism provides much more beneficial effects when it is gradual rather than all at once. As several active pharmaceutical compounds (drugs, vitamins, sugars, etc.) are often semicrystalline and hydrophobic, numerous reports of their erratic oral absorption exist, because of poor dissolution rates in the gastrointestinal fluids. A promising solution to this problem seems physical stabilization of amorphous drug phases in solid dispersions with glassy polymers [1]. Thermodynamically, the drug has a lower chemical potential when mixed with a polymer, resulting in the change of crystallization driving force. One thus achieves a longer time scale of drug's devitrification. Furthermore, when compared with the crystal form, the amorphous form of a poorly water-soluble drug has increased dissolution rates and usually higher bioavailability. Release rates can thus be regulated by appropriate selection of chemical structure, molecular mass [2], and concentration [2–5] of the encapsulating polymer. In parallel, system's efficiency and thermo-physical stability is influenced by the method of preparation [6] and storage conditions (storing temperature and moisture levels) [7, 8].

Correspondence to: Ioannis M. Kalogeras; e-mail: ikaloger@phys.uoa.gr
This article was presented at the POLYCHAR 18 World Forum on Advanced Materials held at the University of Siegen, April 6–9, 2010.
DOI 10.1002/pen.21949
Published online in Wiley Online Library (wileyonlinelibrary.com).
© 2011 Society of Plastics Engineers

The key parameter along the route just described is the knowledge of glass transition temperatures T_g in binary drug + polymer systems. As both the drug and the encapsulating polymer are preferred in an amorphous (glassy) state, crystallization of either component has to be prevented. Hancock et al. [9], for example, proposed that a reasonable guide to stability is to store the pharmaceutical sample at least 50 K below its T_g , near the zero mobility, or Kauzmann, temperature. Long-term crystallization inhibition may be attained in solid dispersions of the drug in a polymer—as opposed to their physical mixtures [6, 10]—where strong steric hindrances and specific intermolecular interactions take place [3, 4, 11]. For example, Konno and Taylor [12] ascribe the reduction in the nucleation rate for crystallization exhibited by felodipine (FEL) in polyvinyl pyrrolidone (PVP), hydroxypropyl methylcellulose (HPMC), and hydroxypropyl methylcellulose acetate succinate (HPMCAS) to an increase in the kinetic barrier for nucleation; the scale of the effect is related to polymer concentration. Moreover, the inhibition can be achieved via antiplasticizing effect of the polymeric component; in other words and in obvious notation, $T_{g,\text{blend}} > T_{g,\text{drug}}$ [4, 13]. The behavior of the ketoconazole (KET) + PVP K-25 solid dispersions studied by Van der Mooter et al. [8] is a sound example. The above factors determine miscibility of the components, which in turn is dictated by the thermodynamics of mixing. The entropy of mixing is always favorable (an increase on mixing) providing one driving force facilitating mixing. Another important factor that affects the miscibility is the enthalpy of mixing. The enthalpic component of the Gibbs function of mixing is controlled by the relative strength of the cohesive drug + drug, polymer + polymer, and the drug + polymer inter-component interactions. Understanding the above relationships is important for optimization of the formulation in drug-delivery systems. The glass transition temperature values tell us a difference between high (accelerated recrystallization, undesirable) and low (stabilized amorphous state) molecular mobility. Varying mass concentration ϕ of the drug in drug + polymer systems causes profound changes in thermophysical properties. These properties are often studied jointly with Fourier-transform infrared spectroscopy (FT-IR).

Analysis of the behavior of the glass transition temperatures of solid dispersions of pharmaceutical compounds in relation to blend composition [$T_g(\phi)$ plots] is thus necessary for production of capsules or tablets with small size and long-term stability. In this work, we have determined $T_g(\phi)$ diagrams for selected drug + polymer systems to provide quantitative results characterizing drug encapsulation. The polymer was in all cases the same, the pharmaceutical grade P(VP-co-VA) copolymer (60 mol% vinyl pyrrolidone and 40% vinyl acetate), known under the trade name Plasdone S-630 Copovidone or PLS-630. It was combined in turn with four poorly water soluble drugs of different properties and biomedical functions: carvedilol (a nonselective adrenergic receptor blocker,

indicated in the treatment of mild-to-moderate congestive heart failure), itraconazole (an antifungal agent that impairs ergosterol synthesis, used among others against histoplasmosis, cryptococcal meningitis, and aspergillosis), nevirapine (a potent, non-nucleoside reverse transcriptase inhibitor used for treatment of HIV infection and AIDS), and nimodipine (a calcium channel blocker with preferential cerebrovascular activity). Solid solutions of the above drugs in PLS-630 were investigated by differential scanning calorimetry (DSC) and FT-IR spectroscopy to evaluate components miscibility, crystallization inhibition, and the extend of intermolecular interactions. Changes in the shape of the $T_g(\phi)$ diagrams and the applicability of important equations (see following section) in their description were examined. The results are presented below, also in relation to other thermophysical characteristics.

$T_g(\phi)$ Functions

A number of equations representing $T_g(\phi)$ relationships for binary (1 + 2) organic systems and copolymers have been developed [14–22] and applied—with variable success—in drug + polymer systems. Fairly often used in binary pharmaceutical systems is the Gordon-Taylor (GT) equation [14]

$$T_g = \frac{\phi_1 T_{g,1} + k_{GT}(1 - \phi_1) T_{g,2}}{\phi_1 + k_{GT}(1 - \phi_1)} \quad (1)$$

which assumes additivity of the specific volumes of the components. ϕ_i , ρ_i , and $T_{g,i}$ are the weight fraction, the density, and the glass transition temperature, respectively, of each component ($T_{g,1} \leq T_{g,2}$; $\phi_1 + \phi_2 = 1$). This equation is valid in case of volume additivity, implying that mixing of molecules of Type 1 and Type 2 does not lead to a volume contraction or expansion. This only holds if the homomolecular interactions are of similar strength as the heteromolecular intermolecular forces. Parameter k_{GT} is claimed to represent the ratio of the free volumes of the two components [14], but is given by [22]

$$k_{GT} = \rho_1 \Delta\alpha_1 / \rho_2 \Delta\alpha_2 \approx \rho_1 T_{g,1} / \rho_2 T_{g,2} \quad (2)$$

where $\Delta\alpha_i$ is the change in the thermal expansivities of each component at the respective T_g . Obviously the claim is unjustified because densities correspond to total specific volumes of the materials not to free volumes; bear in mind [23, 24] that

$$1/\rho = v = v^* + v^f \quad (3)$$

where v^* is the hard-core (incompressible) volume and v^f is the free volume. In most cases, the pretense is dropped and k_{GT} is used as a free fitting parameter.

There is also the Fox equation [15]

$$\frac{1}{T_g} = \frac{\phi_1}{T_{g,1}} + \frac{1 - \phi_1}{T_{g,2}} \quad (4)$$

and the so-called simple rule of mixtures

$$T_g = \phi_1 T_{g,1} + (1 - \phi_1) T_{g,2} \quad (5)$$

both possessing the advantage that only T_g values for pure components are needed in the calculations. Predictions of the $T_g(\phi)$ pattern are also possible through the Couchman-Karas equation [16]

$$\ln T_g = \frac{x_1 \Delta C_{p,1} \ln T_{g,1} + \Delta C_{p,2} (1 - x_1) \ln T_{g,2}}{x_1 \Delta C_{p,1} + (1 - x_1) \Delta C_{p,2}} \quad (6)$$

in which, x_i and $\Delta C_{p,i}$ are the molar fraction and the difference in the heat capacity of the liquid and the heat capacity of the glass forms, respectively. Unfortunately, the application of the aforementioned functions in binary pharmaceutical compound + polymer systems lead to smooth, monotonous $T_g(\phi)$ dependences, that as a rule, either substantially overestimate [2, 4, 7, 25–29] or underestimate [11, 30–32] the experimental ones.

Better in terms of representing strong or asymmetric shapes of $T_g(\phi)$ diagrams, including a few types of s-shaped dependencies, appears to be the Kwei equation [17]

$$T_g = \frac{\phi_1 T_{g,1} + k_{Kw} (1 - \phi_1) T_{g,2}}{\phi_1 + k_{Kw} (1 - \phi_1)} + q \phi_1 (1 - \phi_1) \quad (7)$$

This contains beyond *Eq. 1* a quadratic term after rearrangement, with an empirical interaction-dependent parameter (q). Conformational entropy changes upon mixing are believed to be accounted for by addition of higher order terms such as those appearing in the Brekner-Schneider-Cantow (BSC) equation [18, 20]

$$T_g = T_{g,1} + (T_{g,2} - T_{g,1}) [(1 + K_1) \phi_{2c} - (K_1 + K_2) \phi_{2c}^2 + K_2 \phi_{2c}^3] \quad (8)$$

with

$$\phi_{2c} = k \phi_2 / (\phi_1 + k \phi_2); \quad k \approx T_{g,1} / T_{g,2} \quad (9)$$

Parameter K_1 mainly accounts for the differences between the interaction energies of the binary heteromolecular and homomolecular interactions, whereas parameter K_2 is considered to comprise energetic effects induced by conformational changes (i.e., contributions from conformational entropy changes due to hetero-contact formation). Both parameters contain different amounts of both enthalpic and entropic contributions rendering difficult a straightforward interpretation of their values.

In spite of this, poor representation of experimental patterns is regularly reported in cases of nonrandom

mixing; specific interactions leading to both composition-dependent enthalpic and entropic changes are the source of highly irregular $T_g(\phi)$ patterns [12, 33–35]. The above problems led us to development of the following formula

$$T_g = \phi_1 T_{g,1} + (1 - \phi_1) T_{g,2} + \phi_1 (1 - \phi_1) [a_0 + a_1 (2\phi_1 - 1) + a_2 (2\phi_1 - 1)^2] \quad (10)$$

hereafter denoted as BCKV equation [21]. The quadratic polynomial on its right side, centered around $2\phi_1 - 1 = 0$, is defined to represent deviations from linearity; i.e., with $a_0 = a_1 = a_2 = 0$, the equation leads to the simple rule of mixtures. *Equation 10* transforms to the Jenckel-Heusch equation [36] when only $a_0 \neq 0$. The type and level of the observed deviation is primarily described by parameter a_0 , whereas parameters a_1 and a_2 reflect the strength of asymmetric contributions. Based on comparisons among the results obtained for numerous binary polymer systems [22, 33], using *Eq. 10* and previous $T_g(\phi)$ functions, the empirical parameter a_0 and its normalized form, $a_0/\Delta T_g$ ($\Delta T_g = T_{g,2} - T_{g,1}$), mainly reflects differences between the interaction energies of the hetero- (intercomponent) and homo- (intracomponent) interactions. In proof of that, dependencies have been established among a_0 and the prime parameters of the most common fitting functions (e.g., K_{GT} or q [33]). The magnitude and sign of the higher order fitting parameters of *Eq. 10* is in part related to the system- and composition-dependent energetic contribution of hetero-contacts, entropic effects and structural nano-heterogeneities (e.g., nanocrystalline phases) observed in some blend compositions [22, 33]. Therefore, the number and magnitude of the parameters required to represent an experimental $T_g(\phi)$ pattern provide quantitative measures of system's complexity.

EXPERIMENTAL SECTION

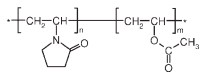
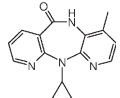
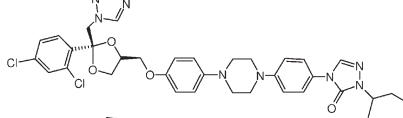
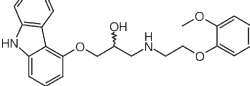
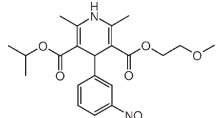
Materials

Carvedilol and Nevirapine were provided by Aurobindo Pharma (Hyderabad, India) as gift samples (Table 1). Nimodipine was obtained as a gift sample from Sun Pharmaceuticals (Vadodara, India). Itraconazole was procured from Letco Medical (Decatur, AL). Plasdone S-630 copovidone was provided as a research sample by ISP technologies (Wayne, NJ).

Sample Preparation

Drug and polymer physical mixtures were prepared in 1.0 g quantities by geometrical mixing in various ratios and further vortex mixed for 2–3 min. Before measurements, the samples were stored at room temperature in glass vials placed in desiccators, containing silica gel or P_2O_5 . Solid dispersions of the different samples were

TABLE 1. Densities ρ , molecular masses M_w , glass transition temperatures T_g , changes ΔC_p in heat capacities at T_g , melting temperatures T_m and enthalpies ΔH_m , and molecular structures of the chemicals.

Chemical	ρ (g/cm ³)	H ⁺ donor sites	H ⁺ acceptor sites ^a	M_w (g/mol)	T_g (K) ^b	ΔC_p (J/g °C)	T_m (K) ^b	ΔH_m (J/g)	Molecular structure
Plasdone S-630 copovidone (PLS-630)	1.162	0	2	24,000–30,000	371.2	2.52	—	—	
Nevirapine (NEV)	1.387	1	5	266.3	362.3	5.01	518.5	1388	
Itraconazole (ITZ)	1.352	0	14	705.6	331.5	3.77	440.4	819	
Carvedilol (CVD)	1.275	3	6	406.5	313.9	9.31	388.6	1148	
Nimodipine (NMP)	1.275	1	9	418.4	288.3	4.78	397.7	916	

^a For PLS-630, the number refers to H⁺ acceptor sites per VP and VA monomer (see following discussion).

^b The standard deviation in the measurement of T_g or T_m is within ± 0.5 K.

prepared within the differential scanning calorimeter, by melting the physical mixtures in the course of the first heating scan performed from room temperature to 200–270°C (heating rate 10°C/min), and subsequently cooling the melt to –20°C at a rate 5°C/min.

Density Measurements

The true density of the samples was determined (in duplicate) using a gas displacement pycnometer (model no. Accupyc 1330, Micromeritics, Norcross, GA).

Fourier-Transform Infrared Spectroscopy

Infrared spectra of selected dried samples were obtained using an FT-IR apparatus (Nicolet IR 100, Thermo Scientific, USA). The formulation sample was mixed with 100-fold KBr for preparing the pellets. The final spectra were composed of 128 scans performed in range 400–4000 cm⁻¹ with 2 cm⁻¹ resolution.

Differential Scanning Calorimetry

Thermal events were studied using a Q200 differential scanning calorimeter (TA Instruments, New Castle, DE) with a refrigeration cooling system (RCS) in a standard mode. Nitrogen was the purge gas at a flow rate of 50 ml/min. The samples (6–10 mg) were weighed in aluminum pans and subjected to heat-cool-heat cycle for the T_g determination. The single T_g values reported here corre-

spond to the midpoint temperature of the heat capacity change recorded during the second heat cycle (averages of at least 2 measurements). The scanning rate employed was 10°C/min for heating and 5°C/min for cooling. Scanning temperature range was from 25 to 200°C and then from 200°C to –20°C, and finally from –20°C to 200°C. In the case of Nevirapine the samples were heated up to 270°C because the drug melting point is near 240°C.

RESULTS AND DISCUSSION

Excess Volumes

Figure 1a shows the results of the true density measurements performed for the pure drugs, the amorphous polymer, and their mixtures. The data reveal a drastic positive deviation of the experimental densities from the expected mass-averaged linear density variation. A more meaningful representation of the data emerges by plotting the excess volume of mixing per g of the sample mass (Fig. 1b),

$$V^E = V_{\text{exp}} - V_{\text{lin}} \quad (11)$$

where the experimental and linear specific volumes were obtained using the relations $V_{\text{exp}} = 1/\rho$ and $V_{\text{lin}} = \phi_1/\rho_1 + (1 - \phi_1)/\rho_2$, respectively (subscripts: 1 for drug, 2 for PLS-630).

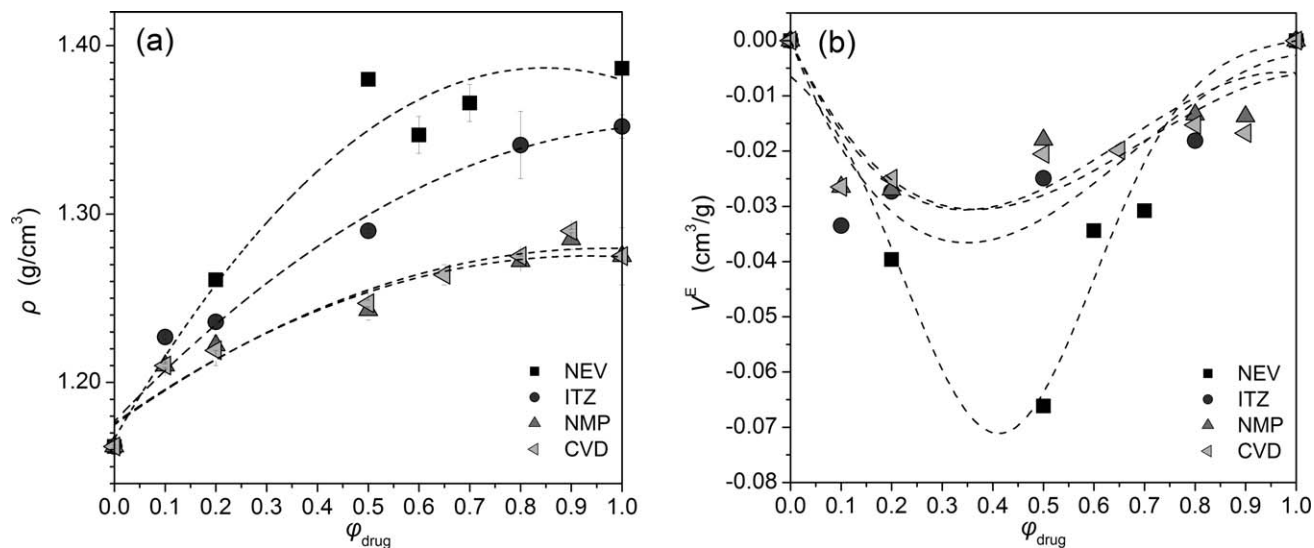


FIG. 1. Compositional variation of: (a) mixture density and (b) the excess mixing volume per gram of sample's mass. The bars account for the standard deviation of the data.

A persistently negative excess mixing volume is seen throughout the entire range of blend compositions. With the exception of the NEV + PLS-630 system, the maximal structural contraction is attained at early stages of drug's addition (ϕ_{drug} up to 0.2). Two effects are presumed to act here. The first is penetration of the drug into structural microscopic voids in the structure of the neat polymer; $V^E < 0$ is the result, apparently a dominating effect. Partial amorphization of initially crystalline drug should result in $V^E > 0$, apparently a minor effect here.

FT-IR Analysis

Components miscibility and thermal stability in binary polymer-containing systems are usually related to strong specific interactions, namely hydrogen-bonding (δH) and ionic ones. Molecular structures of our chemicals suggest the formation of δH interactions between some of our drug molecules (acidic N—H and O—H groups in CVD; N—H groups in NEV and NMP; no H^+ donor groups in ITZ) and the polymeric component (basic C=O groups in PLS-630 Copovidone).

In Fig. 2, we show FT-IR spectra of pure CVD, PLS-630, and their 1:1 physical mixture (PM) and solid dispersion (SD). We note the carbonyl stretching region ($1500\text{--}1800\text{ cm}^{-1}$) and the OH and NH stretching region ($3150\text{--}3450\text{ cm}^{-1}$). Carvedilol has three H^+ donor groups per molecule (as contrasted to no or one acidic group in the other compounds), which can inter-associate with either the cyclic amide C=O groups of vinyl pyrrolidone or the C=O groups of vinyl acetate monomers in Copovidone. Irrespective of the type of mixing (PM or SD), the spectral position of the skeleton stretching vibrations of the C=C bonds [$\nu(C=C)$ at

$1504, 1591, \text{ and } 1608\text{ cm}^{-1}$] in the aromatic ring of Carvedilol ($1502\text{--}1608\text{ cm}^{-1}$ region), as well as the C—H stretching vibrations ($3000\text{--}3100\text{ cm}^{-1}$) and the out-of-plane or in-plane aromatic bending vibrations (at lower wavenumbers [37], not shown here for brevity) remain unaffected by polymer addition. More importantly, in the physical mixtures, no changes in the NH [$\nu(\text{NH})$ at 3308 cm^{-1}] and OH [$\nu(\text{OH})$ at 3346 cm^{-1}] stretching vibration frequencies of CVD appear in the $3150\text{--}3450\text{ cm}^{-1}$ region. These bands are relatively weak, suggesting a limited degree of interactions of the proton donating groups of carvedilol ($>\text{NH}$ and $-\text{OH}$) and the proton accepting carbonyls in PLS-630. We note, however, a clear split of the dual C=O stretching vibration signal of Copovidone—apparent only in the

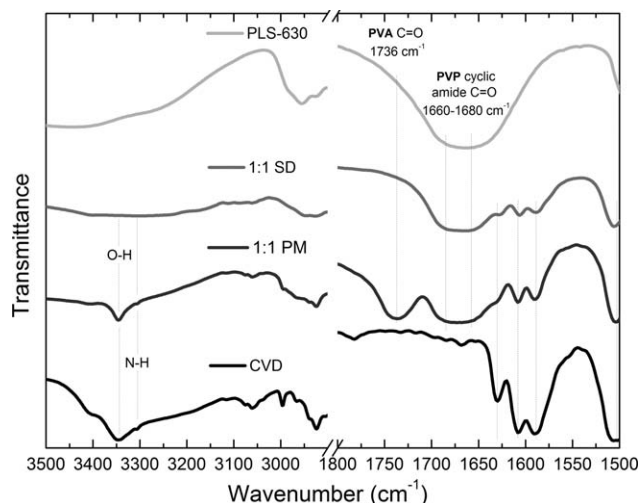


FIG. 2. Part of the FT-IR spectra recorded for CVD, PLS-630, and the physical mixture (PM) and solid dispersion (SD) of the 1:1 CVD + PLS-630 composition.

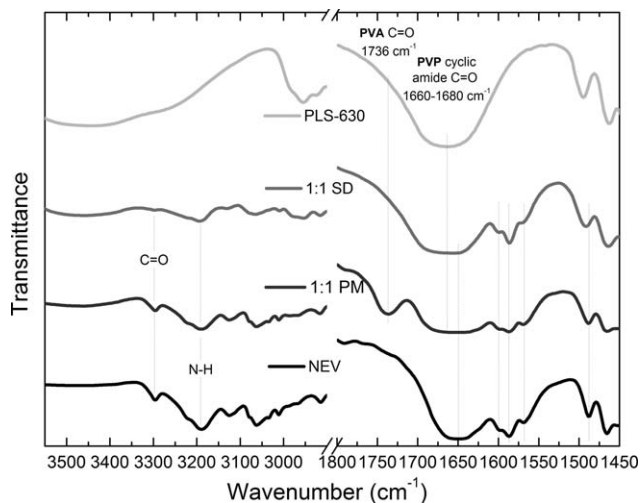


FIG. 3. Part of the FT-IR spectra recorded for NEV, PLS-630, and the physical mixture (PM) and solid dispersion (SD) of the 1:1 NEV + PLS-630 composition.

physical mixture. In the solid dispersion, the 3308 cm^{-1} and 3346 cm^{-1} bands of the drug complex disappear completely, apparently reflecting strong intercomponent interactions.

The vibrational spectra of Nevirapine (Fig. 3) are also of interest. One expects a competition of the C=O groups present both in Copovidone and NEV for hydrogen bonding interaction with proton accepting NH groups in the drug. Thus, a drastic weakening of the broad NH stretching mode of NEV, $\nu(\text{NH})$ observed at 3190 cm^{-1} , is seen in the solid dispersion environment. An analogous conclusion can be extracted from spectral shifts of characteristic deformation signals. Ayala et al. [38] report that a band ascribed to out-of-plane deformation of the NH and the C=O bonds, calculated using density functional theory methods to appear at 726 cm^{-1} , shifts to 804 cm^{-1} as a result of hydrogen bonding and the formation of centrosymmetric molecular dimers. The 804 cm^{-1} band is present in pure NEV and its 1:1 physical mixture, but disappears in the solid dispersion (the diagram not shown here for brevity). The NEV band placed around 3300 cm^{-1} (previously assigned to the first overtone of the $\nu(\text{C}=\text{O})$ band at 1650 cm^{-1}) completely vanishes in the solid dispersion, whereas there is a strong overlap of the C=O bands in the $1500\text{--}1800\text{ cm}^{-1}$ region. The hydroxyl band, with $\nu(\text{OH})$ at 3503 cm^{-1} , characteristic of the pseudopolymorphic (hemihydrate) crystalline form of NEV [38], is absent in our spectra. Therefore, the crystalline fraction of the drug in both the physical mixes and the solid dispersions is most likely organized in the anhydrous (Type I) crystalline form.

DSC Results

A general feature of the second heating DSC traces for our blends is the presence of a single glass transition

signal at each blend composition; in immiscible systems one would detect two glass transitions. We recall that a T_g value is merely a convenient representation of a temperature range, and that the glass transition is not a first order transition (Paul Ehrenfest terminology). The above observation suggests nonequilibrium miscibility in all systems and compositions under study. The term “nonequilibrium” underlines the fact that below T_g the stability of such solid dispersions relies heavily on the kinetics of phase separation and/or crystallization instead of thermodynamics [39]. In the glassy state ($T \leq T_g$) molecular mobilities are drastically suppressed; polymer chain conformations are practically frozen to a nonequilibrium “high energy” state and drug’s (re)crystallization proceeds slowly [39, 40].

Compositional variation of the respective glass transition temperatures is displayed in Fig. 4. The curves have been obtained using Eqs. 1, 7, 8, and 10; given complex shapes of $T_g(\phi)$ diagrams, other equations were not usable. The respective parameters and the coefficients of determination (R^2) are listed in Table 2. These were obtained by applying a Levenberg-Marquardt least-square minimization routine to the experimental data. The GT equation falls short in describing the strongly s-shaped diagrams for solid dispersions of ITZ, NEV, and CVD in PLS-630. The situation slightly improves in the case of the NMP + PLS-630 blend, where the fitting estimate of $k_{GT} = 0.74$ is (within the limits of error) close to its “theoretical” value k_{GT} (and k_{kw}) $\approx \rho_1 T_{g,1} / \rho_2 T_{g,2} = 0.78$. Similar arguments apply also in the case of the Kwei equation. Somewhat better results are obtained using the BSC formula, with the BCKV function providing the highest accuracy in all systems.

The parameters k_{GT} , q (Kwei equation) and a_0 (BCKV equation) progressively decrease in the order: ITZ > NMP > NEV \geq CVD. These parameters are considered semi-quantitative measures of the strength of intercomponent interactions [22], without excluding possible contributions of entropic factors (e.g., the presence of heterogeneities in chains’ packing and conformations, and in large local-density fluctuations) [33]. Given the differences in $\Delta T_g (= T_{g,2} - T_{g,1})$, a more representative indicator of the degree of deviation from linearity is obtained comparing the (dimensionless) reduced $a_0/\Delta T_g$ estimates (Table 2). The maximal positive deviation from the rule of mixtures is observed in the ITZ + PLS-630 system ($a_0, a_0/\Delta T_g > 0$), at a very low drug loading (denoted by the $a_1 \ll 0$ estimate); this is consonant with the highly negative excess mixing volume (V^E) observed in the same compositional region (Fig. 1b). In other words, improved packing hinders movements of polymeric chains and pushes glass transition temperatures upward. In the other systems with $a_0 < 0$, the maximal negative deviation is observed at high drug loading (again $a_1 \neq 0$). Maximal negative deviation is observed in the dispersions of Nevirapine, whereas the Nimodipine solid dispersions demonstrate a behavior very close to the simple rule of mixtures

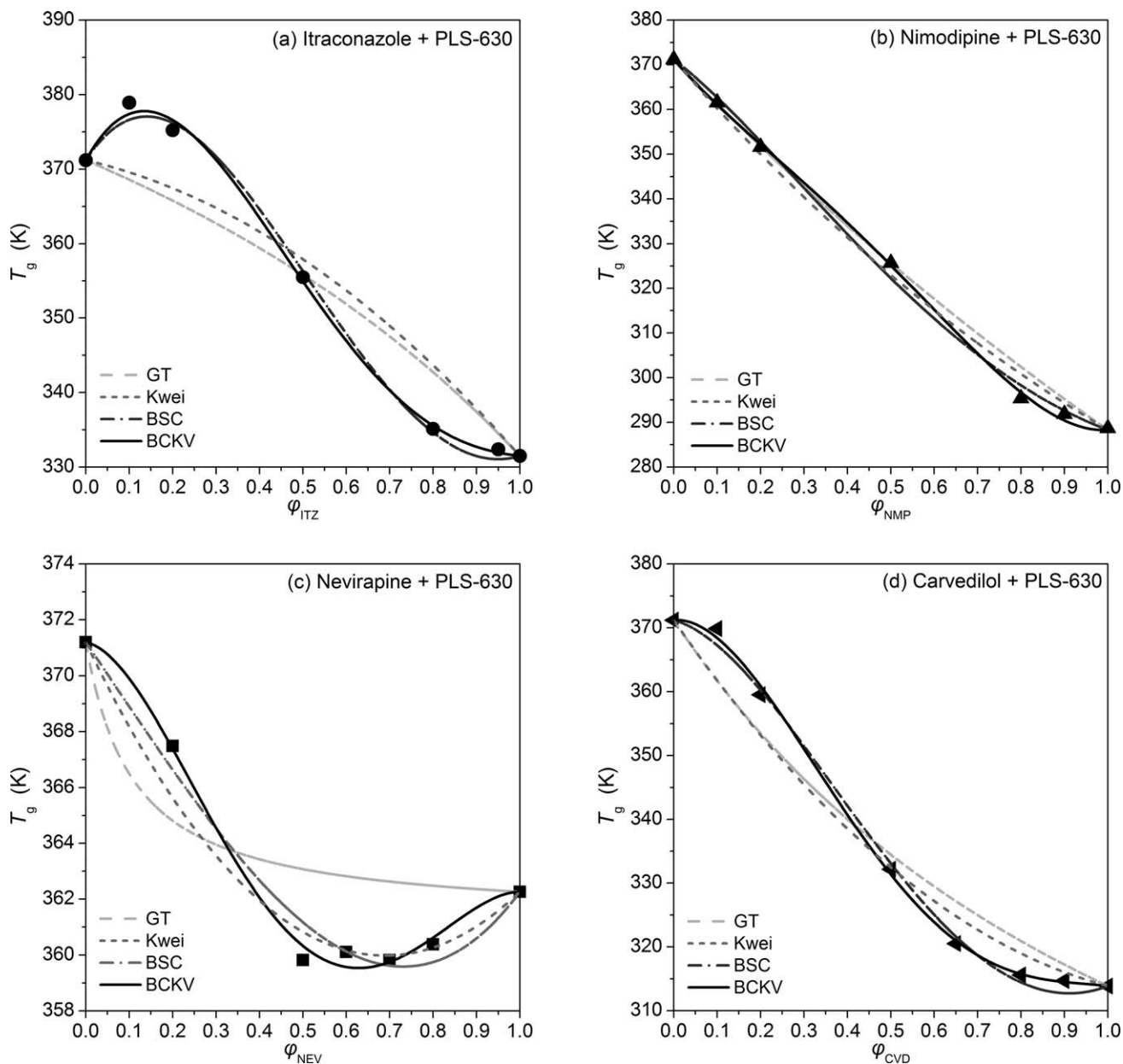


FIG. 4. Compositional variation of blend T_g for the solid dispersions of (a) ITZ, (b) NMP, (c) NEV, and (d) CVD with PLS-630.

(i.e., $a_0/\Delta T_g$ approaches zero). In general at high drug loadings, blend's T_g remains close to $T_{g,drug}$ ($= T_{g,1}$). This is a rather common and not clearly understood behavior encountered in drug + polymer molecular dispersions [4, 11, 25, 26], and is in part reflected also in large values of our a_2 parameter.

In miscible binary blends, the melting point T_m of the crystalline component is usually lower than in pure phase. This is expected due to both morphological and thermodynamic reasons. The former class of reasons comprises changes in the crystal lamella thickness caused by blending, changes in the degree of crystallinity and in physical nature of the amorphous phase surrounding the lamellae. The latter relates to the strength of interactions among

blend components. Melting point depression in our systems is clearly demonstrated in Fig. 5a; it is fairly strong in the mixtures comprising ITZ and NEV and weaker in the CVD or NMP containing mixtures. This suggests a satisfactory degree of mixing among blend components and probably sufficient short-term inhibition of crystallization. The results shown in this figure pertain to physical mixtures, because our solid dispersions are formed by powder's consolidation during the subsequent first cooling scan. The importance of the latter observation lays in our ability to accomplish even more effective long-term crystallization inhibition by using more elaborate mixing techniques (such as spin casting or hot-melt extrusion). There are methods of calculation of equilibrium melting

TABLE 2. Parameters of the $T_g(\phi)$ equations and coefficient of determination (R^2) values.

Equation	Drug molecule			
	ITZ	NMP	NEV	CVD
GT				
k_{GT}	1.6 ± 0.8	0.74 ± 0.07	0.10 ± 0.12	0.56 ± 0.12
R^2	0.9042	0.9914	0.6921	0.9588
Kwei				
k_{kw}	0.89	0.78	0.98	0.85
q	30.9 ± 17.7	-6.5 ± 7.8	-23.4 ± 1.9	-31.0 ± 10.0
R^2	0.9140	0.9937	0.9634	0.9699
BSC				
K_1	-1.51 ± 0.24	-0.43 ± 0.17	-3.4 ± 0.5	-1.54 ± 0.15
K_2	-4.52 ± 0.42	-0.73 ± 0.31	-1.9 ± 1.1	-2.26 ± 0.30
$K_1 - K_2$	3.01	0.30	-1.50	0.72
R^2	0.9967	0.9968	0.9758	0.9968
BCKV				
a_0	14.4 ± 4.2	-18.3 ± 4.2	-25.6 ± 1.2	-44.7 ± 3.2
a_1	-89.7 ± 6.9	-30.2 ± 6.5	-7.3 ± 2.6	-56.0 ± 5.5
a_2	42.0 ± 14.0	-40.8 ± 13.2	23.8 ± 6.1	51.0 ± 11.0
$a_0/\Delta T_g$	+0.363	-0.221	-2.876	-0.780
$a_1/\Delta T_g$	-2.259	-0.364	-0.820	-0.977
R^2	0.9982	0.9994	0.9949	0.9989

diagrams in terms of the Flory-Huggins-Staverman interaction parameter χ_{12} , but these methods are not very accurate [39, 41]. Flory himself proposed a better model of thermodynamic behavior of mixtures taking into account equation of state contributions [23]—a model which provides results of better accuracy, but requires more data [42]. Our melting point depression results suggest $\chi_{12} \leq 0$ (i.e., appreciable attraction between the components)—in agreement with the composition-dependent single- T_g diagrams in our systems.

Amorphous solid dispersions should be prepared preferably at a drug concentration below the solid solubility of its crystalline form, so as to achieve a homogeneous dispersion. If that solubility limit is exceeded, the drug may undergo crystal growth upon storage leading to physical instability of the amorphous solid dispersions [43]. A first indication of polymer's influence on drug crystallization can be extracted by considering the compositional variation of the apparent melting enthalpies ΔH_m per g of sample obtained from the first heating DSC scans. The percentage of drug that remains crystalline in each mixture, $w_{c,drug}$, can be calculated as

$$w_{c,drug} = \frac{\Delta H_m}{\Delta H_m^0} \frac{100}{\phi_{drug}} \quad (\%) \quad (12)$$

where ΔH_m^0 is the apparent (extrapolated) melting enthalpy per 1 g of fully crystalline pure drug. The results obtained using Eq. 12 are presented in Fig. 5b. As expected, the degree of crystallinity of the drug in the freshly prepared drug + polymer physical mixes goes down with increasing concentration of the polymer.

For majority of our blends studied by DSC, no exothermic or endothermic peaks are seen during cooling or the second heating cycle. Thus, the cooling rate of $5^\circ\text{C}/\text{min}$ is in most cases sufficiently high to prevent drug recrystallization on the timescale of the DSC experiment. An exception is pure Nevirapine and some of its blends, which demonstrate a series of rather complex and strongly composition-dependent thermal events. These include a cold crystallization exothermic peak in the 1:1 mixture, broad melting peaks during the first heating scan (particularly for 1:4 and 4:1 drug-to-polymer weight ratios), and crystallization exotherms and melting endotherms during the second heating scan (in pure NEV and in the 1:1 blend only). Evidently,

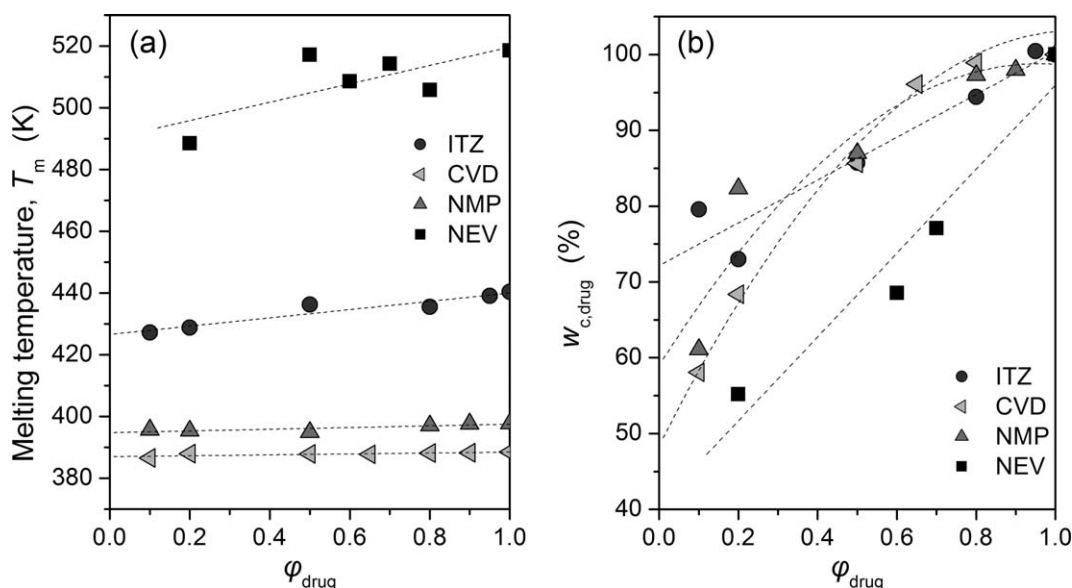


FIG. 5. Compositional variation of (a) the melting temperatures (T_m) and (b) the percentage of drug that exists in a crystalline phase ($w_{c,drug}$), obtained from the first heating DSC scans of the pure drugs and their physical mixtures with amorphous Plasdane S-630 copolymer. Averages of two measurements are reported.

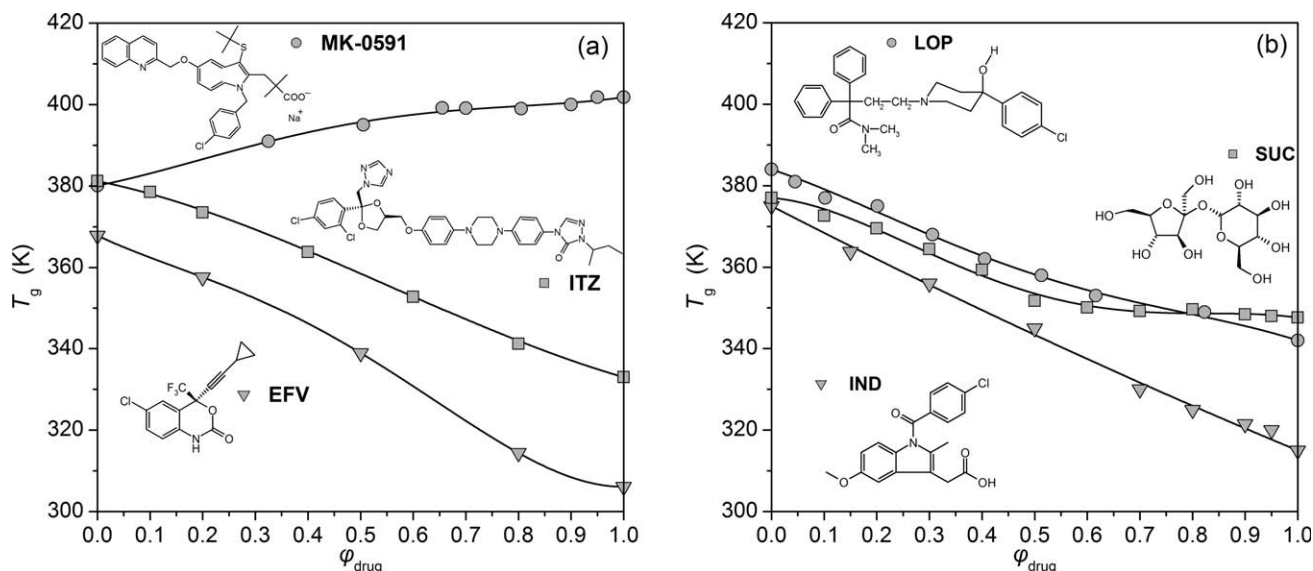


FIG. 6. Compositional variations of blend T_g for solid dispersions of (a) MK-0591, EFV, and ITZ as well as (b) SUC, IND, and LOP drugs in various grades of P(VP-co-VA) copolymers, and their description using the BCKV equation. Drugs' chemical structures are also inserted.

the low rigidity provided by the polymeric component in its blends with Nevirapine (in this case $\Delta T_g = T_{g(\text{PLS-630})} - T_{g(\text{NEV})} \approx +9$ K only) allows for an enhanced drug molecule mobility and easier organization into crystalline phases at low cooling rates. The latter adversely affects drug's solubility; thus, PLS-630 is not a good encapsulant in this case in pharmaceutical oral drug-delivery systems, whether tablets or granules.

The glass transition temperature versus composition dependencies determined here for materials prepared by the fusion method can be combined with previously published results for molecular dispersions prepared by other techniques [4, 11, 25, 32, 34]. In Fig. 6, we show $T_g(\phi)$ relations for solid dispersions of a model drug MK-0591, Sucrose, indomethacin, itraconazole, efavirenz, and loperamide drugs in various grades of P(VP-co-VA) copoly-

mers, and results of the use of the BCKV Eq. 10. The first three blends were prepared using the solvent evaporation technique the following two using the hot-melt extrusion method and the latter by spray drying of appropriate solutions. The parameters obtained using Eqs. 8 and 10 are provided in Table 3. The issue of drug + polymer interactions has been considered by various research groups (e.g., Nair et al. [29] and McGinity and coworkers [2, 28]). The present results indicate that the occurrence of a high number of proton donor sites in the drug molecule is not mandatory for achieving miscibility and crystallization inhibition. For example, $a_0 > 0$ and miscibility is verified in the case of the MK-0591, EFV, and ITZ solid dispersions with P(VP-co-VA) copolymers—in which no (or only one per drug molecule) intermolecular hydrogen bonds are possible. From the data included in

TABLE 3. Mixture information and curve-fitting results for the parameters incorporated in the BCKV equation for literature data on solid dispersions of pharmaceutical compounds in P(VP-co-VA) copolymers (with T_g 's in the range 368–384 K).

Drug	$T_{g,\text{drug}}$ (K)	Functional groups		BSC parameters			BCKV parameters					
		H ⁺ donor sites	H ⁺ acceptor sites	K_1	K_2	R^2	a_0	a_1	a_2	$a_0/\Delta T_g$	$a_1/\Delta T_g$	R^2
MK-0591 [11]	401.8	0	5	1.07 ± 0.25	0.43 ± 0.41	0.9902	19.0 ± 1.8	0	-15.3 ± 8.5	0.873	0	0.9927
Efavirenz (EFV) [34]	306.1	1	3	-0.4 ± 0.2	-0.9 ± 0.1	0.9971	8 ± 1	-32 ± 3	-39 ± 7	0.129	-0.516	1
Itraconazole (ITZ) [32]	332.4	0	12	-0.13 ± 0.06	-0.65 ± 0.11	0.9952	5.6 ± 0.8	-16.6 ± 2.1	0	0.114	-0.339	0.9997
Indomethacin (IND) [4]	315	1	5	0.07 ± 0.05	0	0.9961	-6.4 ± 3.0	0	0	-0.107	0	0.9961
Loperamide (LOP) [13]	342	1	4	-0.28 ± 0.05	0	0.9932	-19.1 ± 2.7	0	18.6 ± 12.4	-0.455	0	0.9947
Sucrose (SUC) [25]	348	8	11	-1.66 ± 0.24	-1.38 ± 0.46	0.9831	-35.1 ± 2.4	-15.3 ± 4.8	39.3 ± 10.7	-1.210	-0.531	0.9921

Tables 2 and 3, it appears that for the dispersions obtained with EFV and ITZ entropic effects supply the major contribution to the observed miscibility; both $a_1/\Delta T_g$ and K_2 are negative, whereas the parameters conveying the strength/influence of enthalpic factors are near zero ($a_0/\Delta T_g$) or even negative (K_1). In the other system, the ion-dipole interaction between the $\text{COO}^- \text{Na}^+$ group of MK-0591 and the cyclic amide group of vinyl pyrrolidone monomer promotes miscibility and drug crystallization inhibition; K_1 , K_2 , and $a_0/\Delta T_g > 0$, in agreement with the above explanation. On the other hand, in the case of the sucrose mixtures hydrogen bonding interactions have been verified by FT-IR spectroscopy studies, whereas we have a strongly negative $a_0/\Delta T_g$. In this case, the magnitude of negative deviation is apparently determined by entropic effects, which counterbalance components' interassociation. In proof of that, Shamblin et al. [25] report $V^E > 0$, of the order of 0.1–1%. The antiplasticizing effect of the polymer matrix has been reported to account for the achieved miscibility and crystallization inhibition in the completely amorphous loperamide + P(VP-co-VA) solid dispersions, in which δH bonds are absent [13]. As seen above, our approach relies particularly on the dependence of glass transition temperatures on composition. The knowledge of $T_g(\phi)$ relations as embodied by parameters of Eq. 10, their signs and magnitudes, allows quantification of usability of a given polymer as an encapsulant for a given drug.

REFERENCES

- D.Q.M. Craig, *Int. J. Pharm.*, **231**, 131 (2002).
- M.O. Omelczuk and J.W. McGinity, *Pharm. Res.*, **9**, 26 (1992).
- L.S. Taylor and G. Zografi, *Pharm. Res.*, **14**, 1691 (1997).
- T. Matsumoto and G. Zografi, *Pharm. Res.*, **16**, 1722 (1999).
- A. Paudel, J. Van Humbeeck, and G. Van den Mooter, *Mol. Pharm.*, **7**, 1133 (2010).
- S. Sinha, S. Baboota, M. Ali, A. Kumar, and J. Ali, *J. Dispersion Sci. Technol.*, **30**, 1458 (2009).
- P.J. Marsac, A.C.F. Rumondor, D.E. Nivens, U.S. Kestur, L. Stanciu, and L.S. Taylor, *J. Pharm. Sci.*, **99**, 169 (2010).
- G. Van den Mooter, M. Wuyts, N. Blaton, R. Busson, P. Grobet, P. Augustijns, and R. Kinget, *Eur. J. Pharm. Sci.*, **12**, 261 (2001).
- B.C. Hancock, S.L. Shamblin, and G. Zografi, *Pharm. Res.*, **12**, 799 (1995).
- P. Di Martino, E. Joiris, R. Gobetto, A. Masic, G.F. Palmieri, and S. Martelli, *J. Cryst. Growth*, **265**, 302 (2004).
- K. Khougaz and S.-D. Clas, *J. Pharm. Sci.*, **89**, 1325 (2000).
- H. Konno and L.S. Taylor, *J. Pharm. Sci.*, **95**, 2692 (2006).
- I. Weuts, D. Kampen, A. Decorte, G. Verreck, J. Peeters, M. Brewster, and G. Van den Mooter, *Eur. J. Pharm. Sci.*, **22**, 375 (2004).
- M. Gordon and J.S. Taylor, *J. Appl. Chem. USSR*, **2**, 493 (1952).
- T.G. Fox, *Bull. Am. Phys. Soc.*, **1**, 123 (1956).
- P.R. Couchman and F.E. Karasz, *Macromolecules*, **11**, 117 (1978).
- T.K. Kwei, *J. Polym. Sci. Lett.*, **22**, 307 (1984).
- M.-J. Brekner, H.-A. Schneider, and H.-J. Cantow, *Makromol. Chem.*, **189**, 2085 (1988).
- A.J. Kovacs, *Adv. Polym. Sci.*, **3**, 394 (1963).
- H.-A. Schneider, *J. Res. Natl. Inst. Stand. Technol.*, **102**, 229 (1997).
- W. Brostow, R. Chiu, I.M. Kalogeras, and A. Vassilikou-Dova, *Mater. Lett.*, **62**, 3152 (2008).
- I.M. Kalogeras and W. Brostow, *J. Polym. Sci. Phys.*, **47**, 80 (2009).
- P.J. Flory, *Selected Works*, Vol. 3, Stanford University Press (1985).
- W. Brostow, *Pure Appl. Chem.*, **81**, 417 (2009).
- S.L. Shamblin, L.S. Taylor, and G. Zografi, *J. Pharm. Sci.*, **87**, 694 (1998).
- S.L. Shamblin, E.Y. Huang, and G. Zografi, *J. Thermal Anal.*, **47**, 1567 (1996).
- J. Berggren and G. Alderborn, *Pharm. Res.*, **20**, 1039 (2003).
- C. Wu and J.W. McGinity, *AAPS PharmSciTech*, **2**, article no 24 (2001).
- R. Nair, N. Nyamweya, S. Gönen, L.G. Martínez-Miranda, and S.W. Hoag, *Int. J. Pharm.*, **225**, 83 (2001).
- P.J. Marsac, H. Konno, and L.S. Taylor, *Pharm. Res.*, **23**, 2306 (2006).
- G.P. Andrews, O.A. Abudiak, and D.S. Ones, *J. Pharm. Sci.*, **99**, 1322 (2010).
- K. Six, G. Verreck, J. Peeters, M. Brewster, and G. Van den Mooter, *J. Pharm. Sci.*, **93**, 124 (2004).
- I.M. Kalogeras, *Thermochim. Acta*, **509**, 135 (2010).
- R.J. Babu, W. Brostow, I.M. Kalogeras, and S. Sathigari, *Mater. Lett.*, **63**, 2666 (2009).
- J. Albers, R. Alles, K. Mattheé, K. Knop, J.S. Nahrup, and P. Kleinebudde, *Eur. J. Pharm. Biopharm.*, **71**, 387 (2009).
- E. Jenckel and R. Heusch, *Kolloid Z*, **130**, 89 (1953).
- L. Jagannathan, R. Meenakshi, S. Gunasekaran, and S. Srinivasan, *Mol. Simul.*, **36**, 283 (2010).
- A.P. Ayala, H.W. Siesler, S.M.S.V. Wardell, N. Boechat, V. Dabbene, and S.L. Cuffini, *J. Mol. Struct.*, **828**, 210 (2007).
- F. Qian, J. Huang, and M.A. Hussain, *J. Pharm. Sci.*, **99**, 2941 (2010).
- J. Tao, Y. Sun, G.G. Zhang, and L. Yu, *Pharm. Res.*, **26**, 855 (2009).
- W. Cheung and R.S. Stein, *Macromolecules*, **27**, 2512 (1994).
- W. Brostow, *Macromolecules*, **4**, 742 (1971).
- J. Huang and R.J. Wigent, *Am. Pharm. Rev.*, **12**, 18 (2009).